Ionic currents of the lateral pyloric neuron of the stomatogastric ganglion of the crab J

Article *in* Journal of Neurophysiology · March 1992

DOI: 10.1152/jn.1992.67.2.318 · Source: PubMed

2 authors:

Jorge Golowasch
New Jersey Institute of Technology
55 PUBLICATIONS **2,307** CITATIONS

SEE PROFILE

Eve Marder
Brandeis University
336 PUBLICATIONS **19,004** CITATIONS

SEE PROFILE

JOURNAL OF NEUROPHYSIOLOGY
Vol. 67, No. 2, February 1992. *Printed in U.S.A.*

Ionic Currents of the Lateral Pyloric Neuron of the Stomatogastric Ganglion of the Crab

JORGE GOLOWASCH AND EVE MARDER
Department of Biology, Brandeis University, Waltham, Massachusetts 02254-9110

SUMMARY AND CONCLUSIONS

1. The lateral pyloric (LP) neuron is an important component of the network that generates the pyloric rhythm of the stomatogastric ganglion (STG) and is a direct target of many modulatory inputs to the STG. Our aim in this and the subsequent two papers is to describe the conductances present in this cell and to understand the role these conductances play in shaping the activity of the neuron.

2. LP neurons were studied in two-electrode voltage clamp (TEVC) in a saline solution containing tetrodotoxin (TTX) and picrotoxin (PTX) to isolate them pharmacologically from presynaptic inputs.

3. We identified six voltage-dependent ionic conductances. These include three outward currents that resemble a delayed rectifier current, a Ca^{2+}-activated K^+ current and an A-current similar to those seen in many other preparations. LP neurons show three inward currents, a fast TTX-sensitive current, a hyperpolarization-activated inward current, and a Ca^{2+} current.

INTRODUCTION

To those who seek to understand how the nervous system generates behaviors, biophysical studies of the ion channels found in neurons of the CNS have provided an embarrassment of riches (Hille 1984). It is now patently clear that the neurons that participate in the generation of complex behaviors will display large numbers of ion channels, many of which are likely subject to modulation by transmitters and hormones (Kaczmarek and Levitan 1987). However, despite the profound insights that biophysics has provided into the structure, function, and modulation of single ion channels, relatively few attempts have been made to understand the contribution of the full complement of conductances displayed by a neuron to its overall excitability properties. Our aim is eventually to understand the biophysical and cellular mechanisms that underlie circuit modulation in the crab stomatogastric ganglion (STG). To this end, we have initiated a study of the ionic currents found in one of the most important neurons in the STG of the crab, *Cancer borealis*, the lateral pyloric (LP) neuron. This paper provides a general description and identification of the ionic currents expressed by this cell.

The LP neuron is multifunctional. It is an excitatory motor neuron that innervates several muscles that participate in the rhythmic constriction of the pyloric chamber of the foregut (Hooper et al. 1986). Additionally, the LP neuron makes a number of inhibitory connections within the neuropil of the STG (Eisen and Marder 1982), where these connections play an important role in shaping the pyloric motor patterns produced by the STG. Many of the neuromodulators of the motor patterns produced by the STG markedly influence the number of LP action potentials fired within each cycle of the pyloric rhythm (Hooper and Marder 1987; Marder et al. 1986; Marder and Weimann 1992; Nusbaum and Marder 1988, 1989a,b). For these reasons, and because there is only a single LP neuron in each ganglion, we chose to study the currents of this neuron.

Many of the currents found in neurons depend critically on both voltage and time, and the expression of each of the currents in a neuron contributes to, and is influenced by, the dynamical properties of the neuron's firing pattern. Therefore we first characterized as many as possible of the voltage- and time-dependent conductances found in the LP neuron. We then constructed a model neuron from these conductances (Buchholtz et al. 1992). In the model neuron we can determine the role of each conductance in shaping the firing pattern of the neuron under a variety of dynamical situations that mimic the activity of the neuron under physiological conditions (Golowasch et al. 1992).

METHODS

Experiments were performed on dissected stomatogastric nervous systems (cf. Selverston and Moulins 1987) from the crab, *C. borealis*, obtained from local fish markets and kept in seawater aquaria at ~12°C. Data were collected from ~50 experiments.

STGs were desheathed, pinned on a silicone elastomer (Sylgard)-lined Petri dish, and cells identified as described in Hooper et al. (1986). Inputs from anterior ganglia were blocked by placing a petroleum jelly (Vaseline) well around the desheathed stomatogastric nerve (stn) filled with isotonic (750 mM) sucrose. Preparations were superfused with *Cancer* saline through a homemade cooling device with the use of thermoelectric heat pumps (Melcor, NJ) to maintain the temperature at 9–11°C. The composition of *Cancer* saline was (in mM) 440 NaCl, 11 KCl, 13 $CaCl_2$, 26 $MgCl_2$, 5 maleic acid, 11 trizma base, and pH 7.4–7.5. When divalent cations were added, Ca^{2+} was removed, retaining at least 0.1 mM Ca^{2+} in the bath to maintain membrane stability. Low amounts of divalent cations (<200 μM) were added without compensation. Less than 10 mM concentrations of other substances (CsCl, TEACl, etc.) were added to the bathing saline without compensation.

Unless otherwise specified, chemicals were obtained from Sigma (St. Louis, MO). They were all prepared immediately before use. Tetrodotoxin (TTX; Calbiochem) was dissolved in distilled water to obtain a stock solution of 10^{-4} M and kept at ~4°C. Charybdotoxin (CTX), which was kept frozen in aliquots of ~1 μM, was a gift from Dr. Christopher Miller.

The LP neuron was impaled with two microelectrodes filled with either 0.6 M K_2SO_4 + 20 mM KCl (10- to 25-MΩ resistance) or 2.5 M KCl (5- to 15-MΩ resistance). An Axoclamp 2A (Axon

Instruments, CA) was used for either two-electrode current clamp (TECC) or for two-electrode voltage clamp (TEVC). Currents were filtered with an eight-pole Butterworth filter (901F, Frequency Devices, MA) and recorded on-line on a Gould 2400 chart recorder (Gould, Cleveland, OH). The voltage clamp was driven, and currents and voltages recorded, stored, and subsequently analyzed on a computer with the pClamp software from Axon Instruments (CA). When a leak subtraction procedure was chosen, the p/n protocol was used (Bezanilla and Armstrong 1977), and the n subpulses were applied in the opposite direction from the test pulse, V_{test}. For TEVC the gain was set to the instrument's maximum ($10{,}000 V_{output}/V_{error}$), and capacitance compensation of the electrodes was used. Shielding of the electrodes or separating them with a grounded plate did not improve the recordings. Ground consisted of a calomel reference electrode (Fisher Scientific, NJ) connected to the bath through an agar bridge (4% agar in 0.6 M K_2SO_4 + 20 mM KCl).

To block outward currents, Cs^+ was injected with the use of 5- to 10-nA current pulses of 0.5 s at 1 Hz through Cs_2SO_4 electrodes (0.6 M Cs_2SO_4 + 20 mM KCl).

Unless otherwise specified, experiments were done in the presence of 0.1 μM TTX and 10 μM picrotoxin (PTX). The impalement of the cells was done before TTX, PTX application for proper identification of the cells (Hooper et al. 1986). Impalement after TTX application in the bath rarely gave satisfactory input resistances (R_{in}). Impalement before TTX application gave R_{in} values between 5 and 20 MΩ (Table 1). Cells with lower R_{in} were discarded.

RESULTS

LP neuron

Each STG contains one LP neuron. Figure 1 shows a drawing of an LP neuron filled intracellularly with Lucifer yellow. LP neurons have a large soma (70–100 μm diam) connected to an extensive dendritic tree through a large-diameter neurite from which emerge a few thick branches and the axon. Fine neurites sprout directly from the thick central process, as well as from the secondary branches.

Typical activity patterns of the LP neuron and its functional antagonist, the pyloric dilator (PD) neuron, are shown in normal physiological saline in Fig. 2*A* (*left*). During rhythmic pyloric activity the LP neuron fires bursts of action potentials that are terminated by inhibitory synaptic potentials from other neurons in the pyloric network. PTX (10^{-5} M) blocks the inhibitory glutamatergic synapses in the STG (Eisen and Marder 1982; Marder and Eisen 1984; Marder and Paupardin-Tritsch 1978). Figure 2*A* (*right*) illustrates that application of PTX effectively blocks the synaptic potentials from other pyloric neurons onto the LP neuron. Therefore our experiments were routinely carried out in the presence of PTX to isolate the LP neuron from virtually all of its chemically mediated synaptic inputs from other pyloric neurons.

TABLE 1. *Passive properties and maximum chord conductance values of the lateral pyloric neuron*

Condition	Average ± SD	n
R_{in}, MΩ	11.6 ± 5.5	37
τ_0, ms	198.9 ± 42.2	15
L_0	1.15 ± 0.34	6
V_{rest} (TTX-PTX), mV	−48.9 ± 6.3	38
$\bar{g}_d$, μS*	0.34 ± 0.10	11
$\bar{g}_{o(Ca)}$, μS*	0.74 ± 0.24	9
$\bar{g}_A$ (V_h = −80 mV), μS*	0.38 ± 0.11	17

TTX-PTX, tetrodotoxin-picrotoxin.
* $\bar{g}_j = i_j/(V - E_K)$; E_K assumed to be −80 mV and j is 1 of the 3 currents.

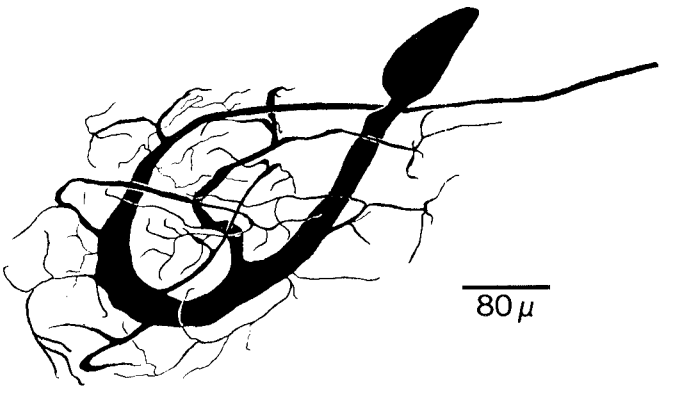

FIG. 1. Drawing of a Lucifer yellow–filled LP cell.

The LP neuron, like the other neurons of the STG, receives modulatory and synaptic inputs from other ganglia via stn fibers that are important in maintaining ongoing rhythmic pyloric activity. The excitatory effects of these inputs can be removed by blocking impulse traffic in the stn (Fig. 2*B*). For further pharmacological isolation, TTX was used to block action potentials (Fig. 2*C*), thus removing spike-mediated synaptic transmission.

Passive properties of the LP neuron

The LP neuron's complex geometry potentially poses space-clamp problems that could make it difficult to achieve good voltage control of the neuron. It has been shown that current injection into the soma of a cell with a geometry like that of the LP neuron (a large, thick neurite with thin processes emerging from it) will show voltage changes that attenuate little as current spreads into the smaller branches as long as the membrane resistance remains relatively constant, whereas the sharpest voltage attenuation usually occurs at the branch points (Graubard and Calvin 1979). This suggests that the soma and the major proximal neurite of the LP cell are nearly isopotential and can be effectively clamped from the soma.

Figure 3*A* shows simultaneous recordings from the soma and a neuropil process at a point several hundred microns from the soma. The slow membrane potential oscillations recorded at these two sites are virtually superimposable, although the fast action potentials are significantly larger at the neuropil recording site than at the soma. This suggests that the fast membrane potential (V) changes are subject to the low-pass filtering that the membrane capacitance imposes on the electrical signals across the membrane. It also indicates that the site of spike initiation is distant from the soma.

Rall and colleagues (Rall 1977) have suggested that cells with an electrotonic length constant, L (approximated by $L = \pi \cdot (\tau_0/\tau_1 - 1)^{-1/2}$, where τ_0 is the membrane time constant and τ_1 the first equalizing time constant), smaller than two to three are electrotonically compact, as long as the membrane resistance remains relatively constant (i.e.,

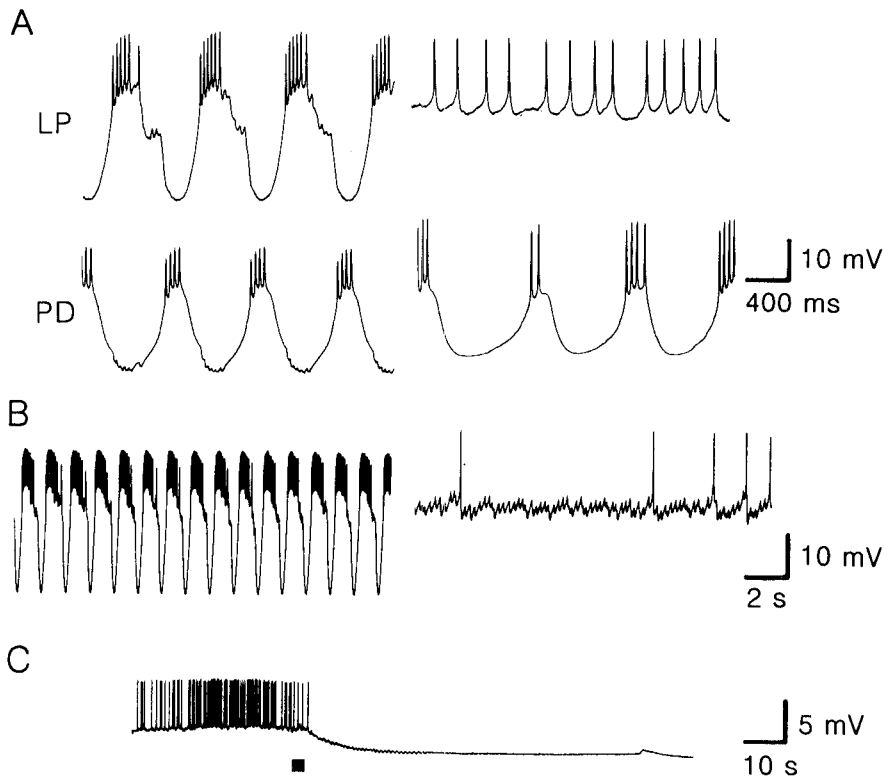

FIG. 2. Isolation of LP cell. *A*: simultaneous intracellular recordings of LP and PD neurons in control saline (*left*) and in 10 μM PTX (*right*). *B*: intracellular recording from LP neuron before (*left*) and after (*right*) applying a sucrose block around the stn to remove afferent inputs. *C*: effect of bath application of 1 μM TTX on a LP cell beginning at the square. The baseline of the action potentials is at $V = -55$ mV.

at steady state). In the experiment illustrated in Fig. 3*B*, two electrodes were placed in an LP neuron, and the voltage responses to constant current pulses are shown. These can be fit by two exponentials (smooth lines in Fig. 3*B*). The shorter time constant, τ_1, is an equalizing time constant, whereas the longer one, τ_0, is the actual membrane time constant (Rall 1977). The equalizing time constant describes the charge movement along the branches of the cell,

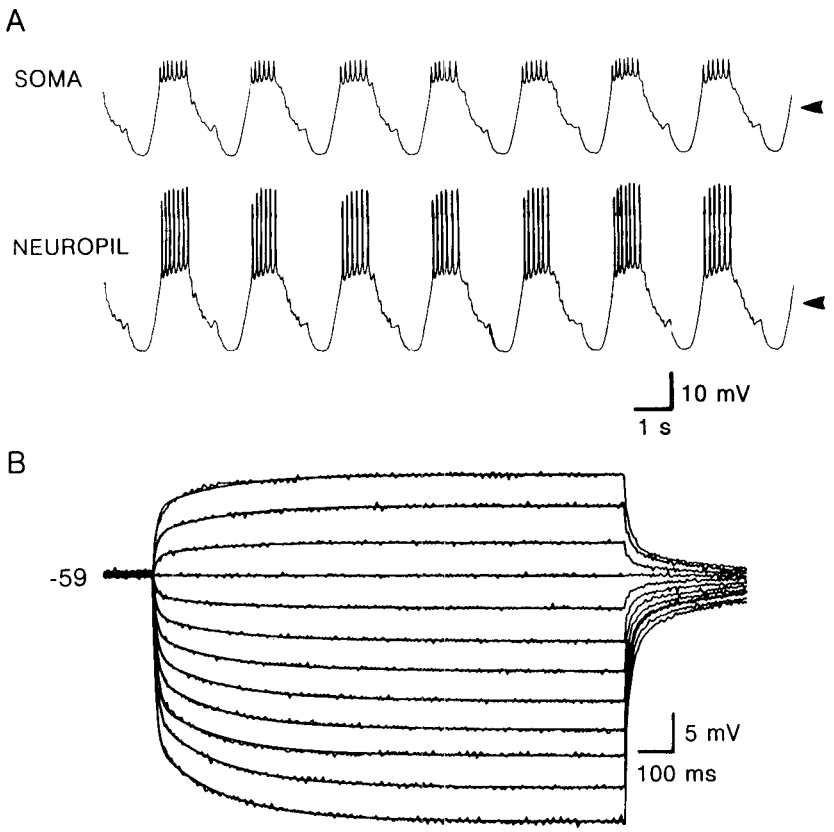

FIG. 3. Cable properties of the LP neuron. *A*: simultaneous intracellular recordings from the soma and neuropil of the LP cell. Preparation in normal saline. Neuropil process impaled ~500 μm away from the cell body. Arrowheads indicate $V = -50$ mV. *B*: voltage responses of an LP cell to constant-current pulses of −8 to +3 nA (steps of 1 nA) in TTX-PTX. Superimposed (smooth traces) are the 2-exponential fits, with $\tau_0 = 212$ ms and $\tau_1 = 11$ ms. Electronic length constant (L_o) = 0.74.

whereas the membrane time constant τ_0 reflects the charge movement across the membrane. By this method, τ_0 was 199 ± 42 (SE) ms. The values of τ_0 and τ_1 obtained for the LP cell indicate that this cell is electrotonically equivalent to a two-compartment model cell with an average electrotonic length constant, L_0 = 1.15 (Table 1). This analysis applies to neurons that can be represented as an equivalent cylinder (Rall 1977), and we have assumed that this is the case for the LP neuron. In most LP cells we were able to measure only two time constants, indicating that after steady-state conditions are achieved we have reasonably good voltage control over most of the membrane in the soma and major processes in spite of their large size.

Outward currents

To characterize the voltage-dependent currents of the LP neuron, experiments were done in TEVC. As seen below, our data indicate that LP neurons display three distinct outward currents that resemble closely the delayed rectifier (i_d), transient A (i_A), and Ca^{2+}-activated outward ($i_{o(Ca)}$) currents described in other preparations. In fact, we employed the well-known properties of i_A and $i_{o(Ca)}$ to isolate each outward current. When depolarizing voltage pulses are applied from a holding potential V_h = −40 mV to remove i_A (see below), two outward current components can be seen (Fig. 4): a fast transient component that inactivates within the first 250 ms, and a slower component that persists for many seconds. Because of the poor voltage control in the first 20–30 ms (Fig. 4, *top*), we never made current measurements in the first 30 ms after the pulse onset. The transient component and part of the sustained component are blocked with 200 μM Cd^{2+} (Fig. 5 and below). We are defining the remaining sustained current that reaches its maximum with a time course that becomes faster as the cell is more depolarized and shows no signs of voltage-dependent inactivation (Fig. 5*A*) as i_d. i_d activates at V values above around −40 mV (Fig. 5*B*), and its maximum chord conductance ($\bar{g}_d$) is ~0.34 μS (Table 1). From the characteristic delayed onset and its voltage dependence, this current resembles other well-described delayed rectifiers (Adams et al. 1982; Czternasty et al. 1989; Hodgkin and Huxley 1952; Thompson 1977). As with most delayed rectifier currents, the steady-state activation $a_\infty(V)$ curve of Fig. 5*B* can be fit with a sigmoidal function. In the present case the following expression adequately fits the data

$$a_\infty(V) = 2.0/\{1 + \exp[(V + 22.4)/-25.9]\}^4$$

Like most delayed rectifier currents (cf. Cobbett et al. 1989; Czternasty et al. 1989; Stanfield 1983; Thompson 1977) the LP i_d is partially blocked by tetraethylammonium (TEA). The block shows a dissociation constant, K_d, of 0.71 mM, assuming a first order of binding and saturates around 10 mM (measured at V_{test} = +20, n = 4). However, the block is not complete and only ~65% of the total i_d is blocked with 10 mM TEA (see Golowasch 1990).

A large component of the outward current that is activated at voltages more positive than V_{rest} is blocked by inorganic divalent cations like Cd^{2+} (Fig. 6, *B* and *D*), Mn^{2+},

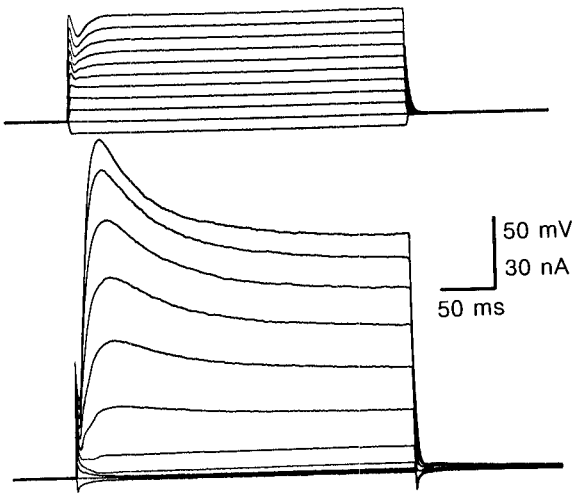

FIG. 4. Outward currents. LP cell in TEVC in TTX-PTX. V_h = −40 mV. V_{test} = −50 to +50 mV in steps of 10 mV. *Top*: voltages recorded by the voltage electrode. Notice the initial deflection in the voltage trace that lasts for ~25 ms. *Bottom*: outward currents in response to voltage steps.

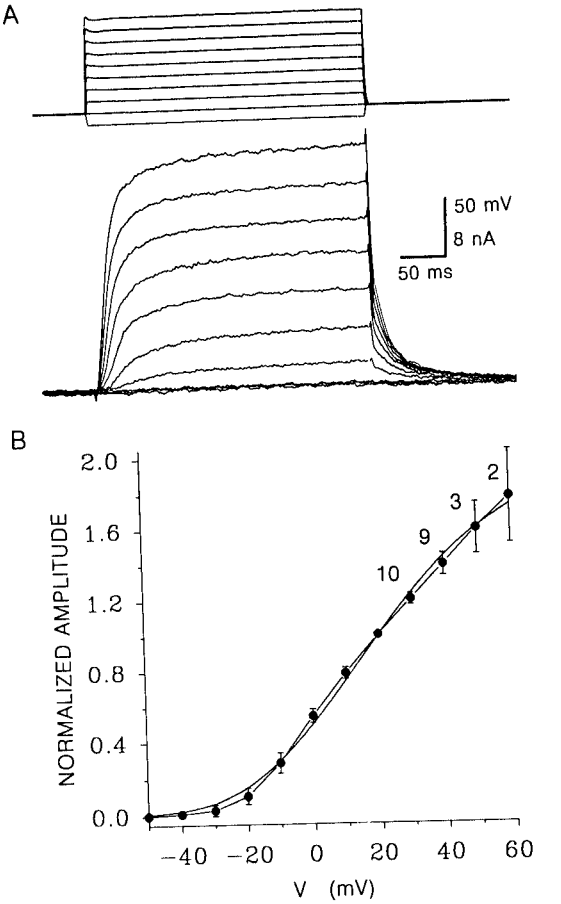

FIG. 5. Voltage dependence of the delayed rectifier, i_d. In TTX-PTX. *A*: currents (*bottom traces*) obtained in the presence of 200 μM Cd^{2+} and measured with *p/n* leak subtraction, n = 5. Voltage (*top*) recorded by the voltage electrode. Notice the improved voltage control by comparison with Fig. 4 (*top*). V_{test} = −50 to +40 mV. *B*: *I-V* plot of currents measured as in *A* in steady-state conditions, typically at 200 ms. Each point is the average ± SD of 12 cells, except where indicated. Normalized to currents measured at V_{test} = +20 mV (31.6 ± 9.3 nA, n = 12). Smooth curve obtained with equation given in the text.

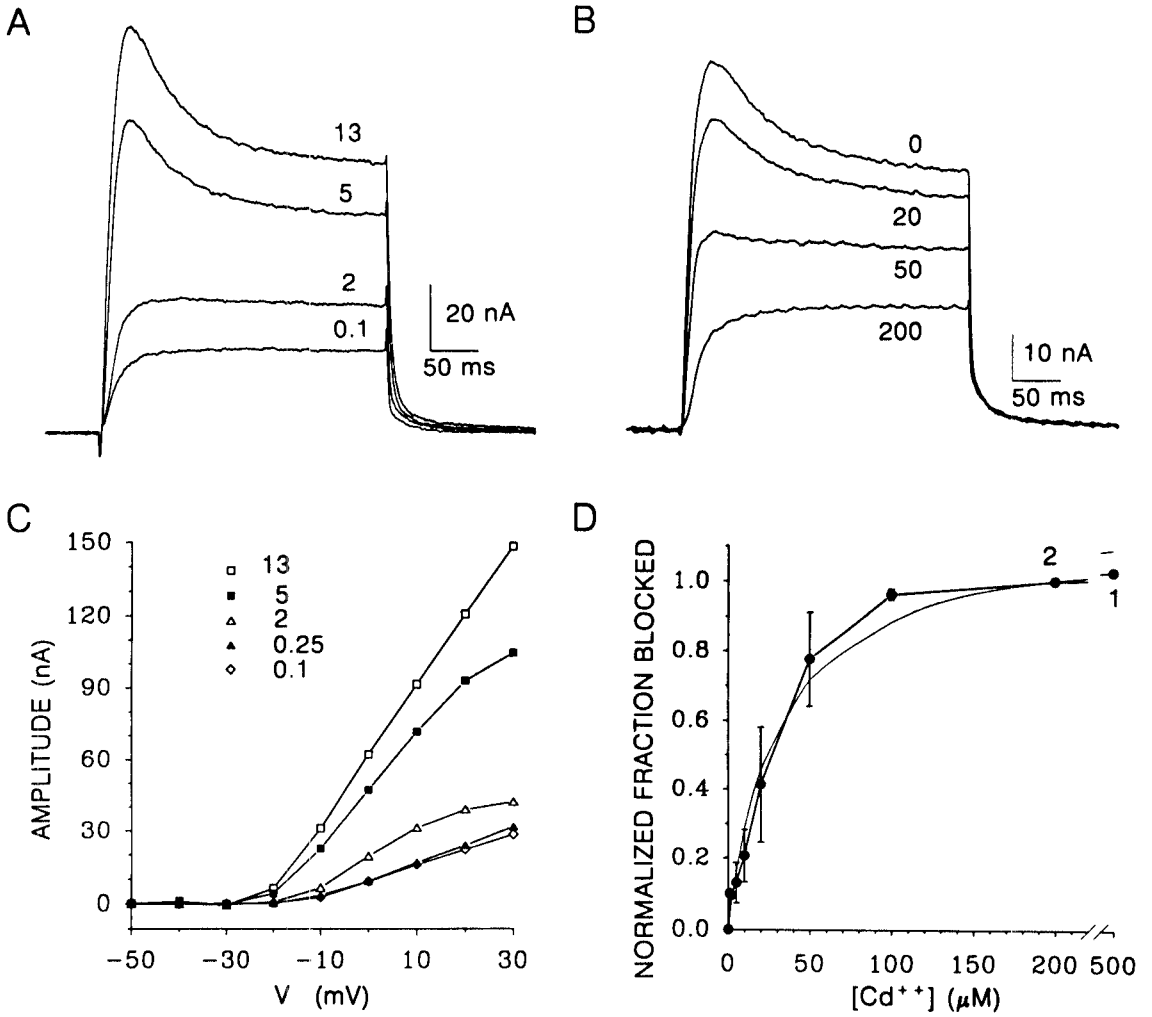

FIG. 6. Sensitivity to divalent cations of the Ca^{2+}-activated outward current, $i_{o(Ca)}$. In TTX-PTX. $V_h = -40$ mV, $V_{test} = +20$ mV. *A*: current traces obtained in different concentrations of extracellular Ca^{2+} (as indicated in mM). Mg^{2+} was substituted for Ca^{2+}. With *p/n* leak subtraction, $n = 5$. The little transients at the end of the pulses are probably an artifact of the leak subtraction procedure because they are never observed when this protocol is not used. *B*: current traces obtained in different concentrations of bath-applied Cd^{2+} (as indicated in μM). With *p/n* leak subtraction, $n = 5$. *C*: *I-V* curve from the data in *A*, measured 40 ms after the onset of the pulse. *D*: concentration dependence of Cd^{2+} blocking effect on $i_{o(Ca)}$ (as shown in *B*). Fraction of total current vs. $[Cd^{2+}]$. Currents normalized to the fraction blocked in 200 μM Cd^{2+} (53.7 ± 12.4 nA, $n = 3$). Average ± SD of 3 cells per point. Smooth curve is the fit to these points assuming 1st-order binding ($K_d = 30.7$ μM). Measurements made at 30 ms after the onset of the pulse.

and Co^{2+}. This component appears to be activated by Ca^{2+} as decreasing the extracellular Ca^{2+} concentration decreases the amplitude of part of the outward current until it reaches a plateau where only the Ca^{2+}-insensitive current is activated, namely i_d (Fig. 6, *A* and *C*). We call the outward current that is sensitive to Ca^{2+} concentrations $i_{o(Ca)}$. $i_{o(Ca)}$ is blocked by increasing concentrations of Cd^{2+} (Fig. 6, *B* and *D*). The blocking effect of Cd^{2+} has a K_d of ~30 μM, assuming first-order binding (measured at +20 mV, $n = 3$). It is this property of Cd^{2+} that we have used to isolate $i_{o(Ca)}$ from i_d (Fig. 5), assuming that Cd^{2+} blocks all of the underlying Ca^{2+} current and that no significant fraction of $i_{o(Ca)}$ remains that can be activated by the existing background Ca^{2+} concentration.

The voltage dependence of $i_{o(Ca)}$ is similar to the voltage dependence of i_d but slightly displaced to more positive voltages: the current traces shown in Fig. 7*A* and the current-voltage (*I-V*) curve of the peak Ca^{2+}-activated outward current in Fig. 7*C* show that it activates at a *V* more depolarized than −30 mV. However, the maximum chord conductance values, ($\bar{g}$) of these two currents differ markedly (Table 1), leaving $i_{o(Ca)}$ as the predominant of the two currents. Like i_d, $i_{o(Ca)}$ does not show signs of voltage-dependent inactivation for voltages more *negative* than −40 mV because there is no difference in amplitude or kinetics in $i_{o(Ca)}$ activated from different V_h values (Fig. 7*B*). This may be, however, a reflection of the voltage-dependent properties of the underlying Ca^{2+} current (see below).

More direct evidence that $i_{o(Ca)}$ is a Ca^{2+}-sensitive current is shown in Fig. 8. Ca^{2+} was injected through a third microelectrode filled with $CaCl_2$, and voltage pulses were applied to +20 mV in control saline during the injection period. With endogenous inward Ca^{2+} currents intact (Fig. 8*A*), the injection of Ca^{2+} has a clear blocking effect on the

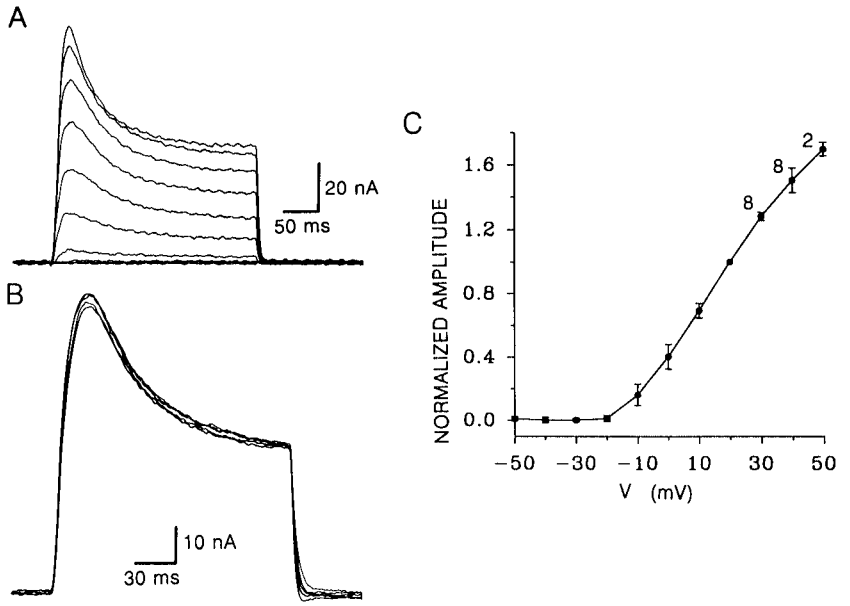

FIG. 7. Voltage dependence of $i_{o(Ca)}$. In TTX-PTX *A*: raw currents obtained by subtracting currents recorded in control saline +200 μM Cd^{2+} from control saline. V_h = −40 mV. V_{test} = −50 to +50 mV. *B*: net Cd^{2+}-sensitive currents obtained in the same way as in *A* but from different V_h levels to a V_{test} = +30 mV. V_h tested: −40, −50, −60, −70, and −80 mV. *C*: *I-V* curve of peak at 30 ms Cd^{2+}-sensitive currents obtained as in *A*. Average ± SD of 9 cells per point except where indicated. Normalized to V_{test} = +20 mV (60.9 ± 17.8 nA, n = 9).

transient part of $i_{o(Ca)}$, suggesting that Ca^{2+} directly inactivates part of $i_{o(Ca)}$. When the endogenous inward Ca^{2+} currents are blocked with Cd^{2+} (Fig. 8*B*), Ca^{2+} injection with positive current pulses induces the activation of a large sustained outward current in response to a depolarizing voltage step to +20 mV, indicating direct Ca^{2+} activation. Thus the apparent transient nature of the Ca^{2+}-activated outward current (Figs. 6–8) seems to be a reflection of the kinetic properties of the underlying Ca^{2+} current and not a property of voltage-dependent inactivation of $i_{o(Ca)}$ itself (cf. Knöpfel et al. 1990). This is best illustrated in Fig. 8*B*, where sustained Ca^{2+} injection activated only a sustained outward current when all the Ca^{2+} currents were blocked with Cd^{2+}.

$i_{o(Ca)}$ is sensitive to TEA, which blocks it almost completely (Golowasch 1990), but insensitive to the bee venom Apamin, known to block a subset of the described Ca^{2+}-activated K^+ currents (Latorre et al. 1989). Nanomolar concentrations of CTX, known to block a set of Ca^{2+}-activated K^+ currents (Latorre et al. 1989), partially and irreversibly blocked $i_{o(Ca)}$ (Golowasch 1990).

Like the originally described i_A of molluscan neurons (Connor and Stevens 1971; Neher 1971), and those described in other species (Rogawski 1985; Cobbett et al. 1989), the LP i_A shows a strong voltage and time dependence of both the activation (Fig. 9, *A* and *B*) and inactivation processes (Fig. 9, *C* and *D*). i_A turns on at voltages around −40 mV (Fig. 9*B*) and steeply increases its activation between −40 mV and approximately +20 mV after which the activation begins to plateau. As previously described (Cobbett et al. 1989; Connor and Stevens 1971; Neher 1971) the voltage dependence of activation is well fit by a sigmoidal function of voltage. The voltage dependence of activation of the LP i_A can be fit with a function, the parameters of which are

$$a(V) = 1.1/\{1 + \exp[(V + 19.4)/-20.3]\}^3$$

Notice, however, that this function describes an approxi-

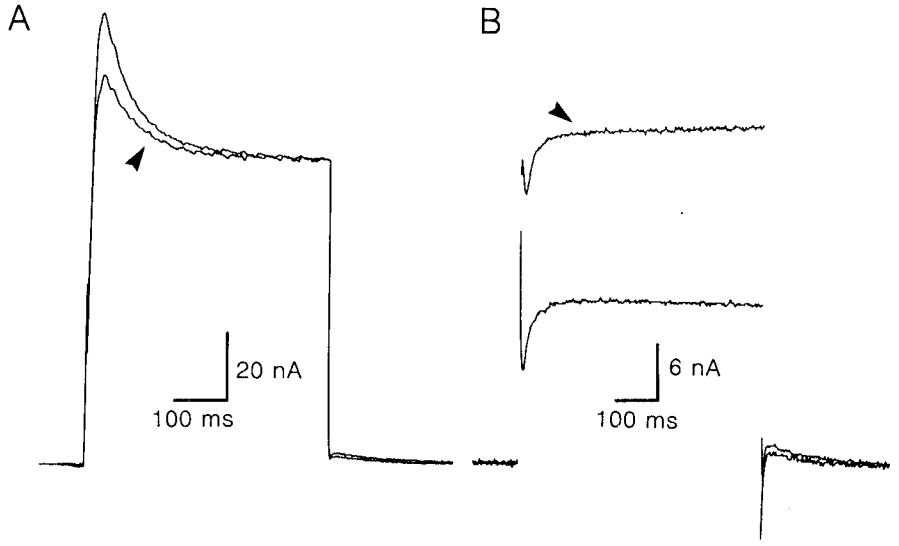

FIG. 8. Sensitivity of $i_{o(Ca)}$ to injected Ca^{2+}. In TTX-PTX. Cell impaled with 3 electrodes; 2 for voltage clamping (K_2SO_4) and 1 containing 80 mM $CaCl_2$. Constant back current of −2 nA was injected through the Ca^{2+} pipette to prevent clogging. Each panel shows the current before and after (arrow) Ca^{2+} injection (+5 nA iontophoretic application). *A*: in control saline. *B*: 200 μM Cd^{2+} was added to the bath to block the endogenous Ca^{2+} currents. All current traces zeroed at the baseline. V_h = −40 mV; V_{test} = +20 mV. No leak or i_d subtraction. Notice the inhibitory effect of Ca^{2+} injection in control saline (*A*) compared with its activating effect when endogenous Ca^{2+} currents are blocked (*B*).

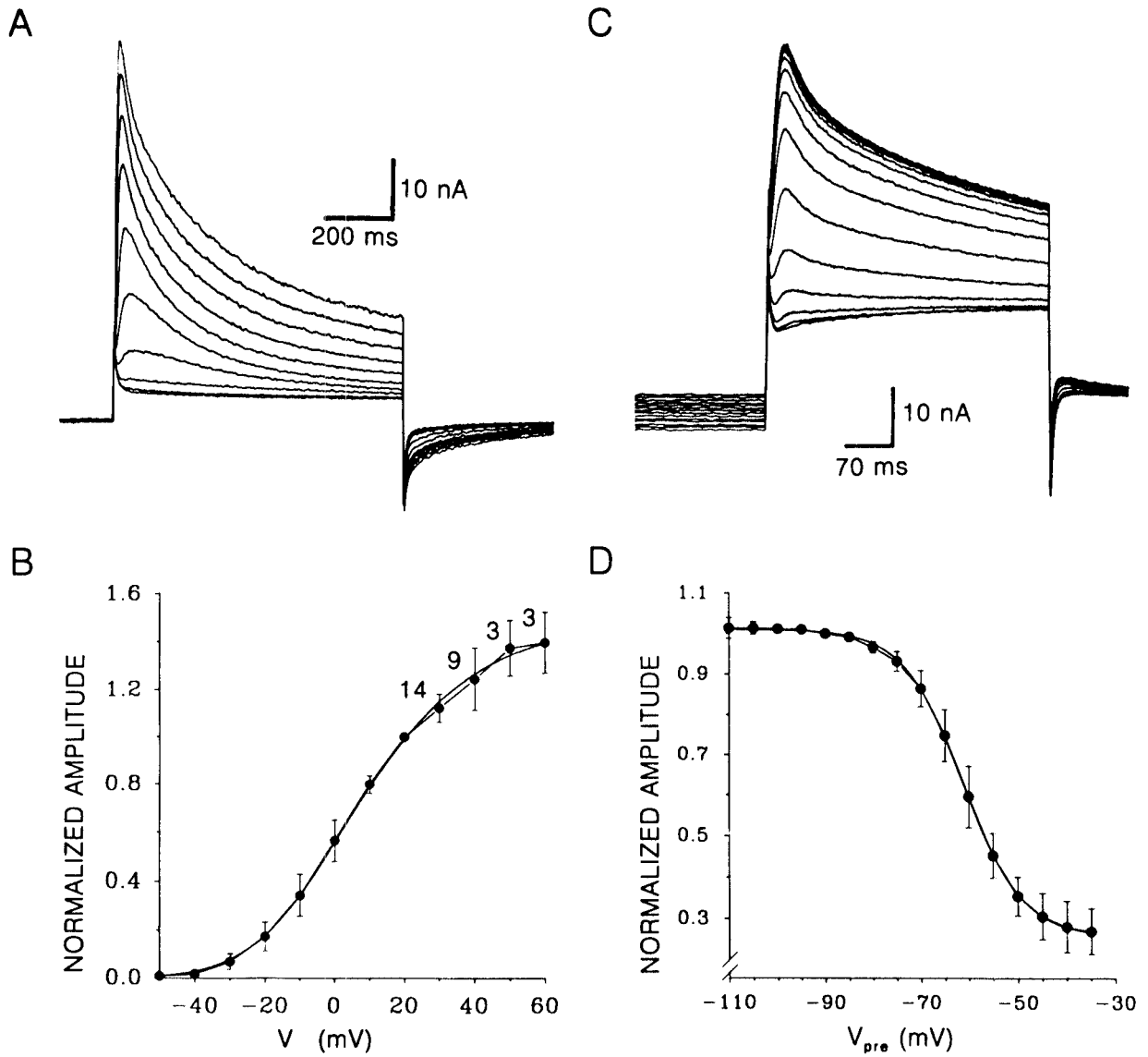

FIG. 9. Voltage dependence of i_A activation and inactivation. TTX-PTX, 200 μM Cd^{2+}, and 10 mM TEA. *A*: activation. Net i_A obtained by subtracting the currents recorded from $V_h = -40$ mV from those recorded from a $V_h = -80$ mV. $V_{test} = -50$ to +40 mV in steps of 10 mV. *B*: *I-V* curve of activation (as in *A*) measured at 30 ms. Average ± SD of 15 cells except where indicated. Currents were normalized to $V_{test} = +20$ mV (38.7 ± 11.7 nA, $n = 15$). *C*: inactivation. Raw current traces to $V_{test} = +30$ mV. $V_h = -40$ mV. Prepulses 2 s long from V_h to voltages ranging from −110 to −35 mV in steps of 5 mV. No leak subtraction. *D*: peak currents measured as in *C* at 30 ms and normalized to the current measured from a prepulse of −90 mV (57.2 ± 10.5 nA, $n = 5$). Each point is the average ± SD of 5 cells. Smooth curves were obtained with the equations given in the text.

mation of the voltage dependence of the true activation because it corresponds to measurements of the peak current at 30 ms. As mentioned below, instantaneous tail current measurements in these cells are not possible, and therefore instantaneous activation and inactivation parameters can not be measured.

The activation kinetics of i_A depend on voltage. i_A activates and reaches a peak more rapidly as the voltage is increased (Fig. 10*A*). i_A is maximally deinactivated at voltages more negative than around −90 mV and completely inactivated at voltages of about −40 mV or higher in the steady state (Fig. 9*D*). As described before (Cobbett et al. 1989; Connor and Stevens 1971; Neher 1971), this inactivation process can be well fit by a sigmoidal function of voltage. The relation in the LP cell is

$$b(V) = 0.26 + 0.75/\{1 + \exp[(V + 61.3)/6.1]\}$$

where 0.26 corresponds to the unsubtracted contribution of i_d to these measurements. The complete inactivation of i_A at around −40 mV is the property we used to separate i_A from the other two outward currents: when voltage pulses from $V_h = -40$ mV are applied, only i_d and $i_{o(Ca)}$ turn on, whereas i_A remains inactive.

i_A inactivation is slow, taking several seconds for the current to decrease to baseline levels. This inactivation process shows two apparent time constants of inactivation

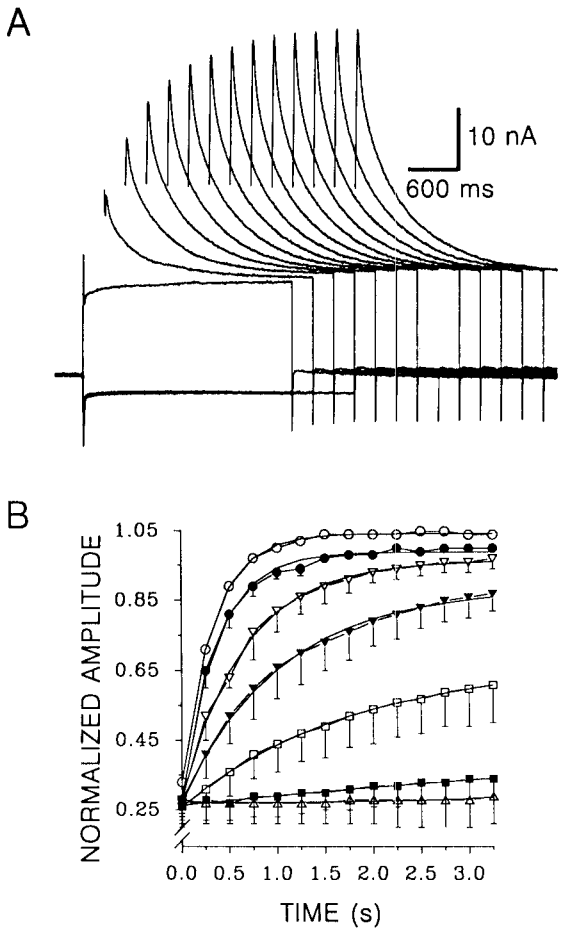

FIG. 10. Time course of the release of the inactivation of i_A. In TTX-PTX + 200 μM Cd^{2+} + 10 mM TEA. V_h = −40 mV. *A*: currents were evoked by a pulse to +30 mV from a prepulse potential of −80 mV and of increasing duration. *B*: peak currents obtained as in *A* at 30 ms after the onset of V_{test} plotted as a function of prepulse duration for different V_{pre} levels (*top to bottom*: −100, −90, −80, −70, −60, −50, and −40 mV). Normalized to the current obtained from a V_{pre} = −90 mV and 3 s of duration (51.9 ± 7.1 nA, n = 3). Each point is the average ± SD of 3 cells.

(Fig. 9*A*), each with a slight voltage dependence that becomes faster as V_{test} is more depolarized (see Golowasch 1990).

The inactivation of i_A can be reversed by hyperpolarizing the cell. The time course of the release of the inactivation (deinactivation) shows a strong dependence on voltage as shown in Fig. 10. In Fig. 10*A* we demonstrate the time and voltage dependence of the inactivation process by applying increasingly longer duration prepulses (V_{pre}) to −80 mV from a V_h = −40 mV. i_A is then activated by stepping the voltage from V_{pre} to a V_{test} of +30 mV (Fig. 10*A*). Figure 10*B* shows that the release of inactivation occurs faster with more negative prepulse voltages, approaching saturation at voltages around −100 mV.

4-Aminopyridine (4-AP) produced a partial and irreversible block of i_A (see Golowasch 1990). 4-AP had limited usefulness for the isolation of ionic currents because it damaged the cells when exposed for too long times even at concentrations that failed to completely block i_A. Short applications were successful but produced incomplete blocking of i_A. The K_d of the 4-AP block of i_A is ~1 mM (measured with a fit assuming 1st-order binding 4-AP, n = 3), suggesting that a large fraction of i_A is blocked with millimolar amounts of the drug. Unlike some other A-like currents reported in the literature (Cobbett et al. 1989; Tasaki and Cooke 1986; Thompson 1977), i_A in the crab is not blocked by TEA. In fact, TEA actually enhanced the apparent rate of activation and the amplitude of i_A, probably because TEA increased R_{in} by blocking i_d and $i_{o(Ca)}$ thus allowing a better voltage control of the cell. Finally, i_A is not affected by Ca^{2+} because neither its activation nor its inactivation characteristics were affected by changing the extracellular Ca^{2+} concentration (not shown).

When the three currents just described were measured in the same cell, the individual ratios of the maximum conductances $\bar{g}_{o(Ca)}/\bar{g}_d$ and $\bar{g}_A/\bar{g}_d$ were 2.2 ± 0.8 and 1.1 ± 0.4, respectively (n = 8). When the averages of the pooled maximum conductances from all measured cells (Table 1) were taken, regardless of whether they were measured in the same cell or not, and the same ratios ($g_{o(Ca)}/\bar{g}_d$ and $\bar{g}_A/\bar{g}_d$) were calculated, identical values were obtained (2.2 and 1.1, respectively).

Inward currents

When the LP is hyperpolarized, a "sag" in the voltage slowly develops that depolarizes the cell. This sag is clearly the result of a conductance activation because R_{in} decreases when the cell is hyperpolarized and the sag is generated (not shown). Underlying this sag is a current (i_h) with the characteristic behavior of an inward rectifier (Angstadt and Calabrese 1989; Arbas and Calabrese 1987; DiFrancesco 1986; Edman et al. 1987; Parker and Miledi 1988), which carries current only inwardly and activates at membrane potentials more negative than V_{rest}. The voltage dependence of i_h activation indicates that it begins activating at −50 to −60 mV and continues to activate toward more negative voltages with no signs of voltage-dependent inactivation (Fig. 11*A, left*). Its steady-state *I-V* curve shows the inward rectifying nature of this current (Fig. 11*B*). Judging from the tail currents obtained at V_H after activating i_h at different voltages (Figs. 11*A* and 12*A*), i_h activation begins to saturate at around −110 mV. Its extrapolated reversal potential is −20 to −30 mV from tail current measurements at different voltages after a prepulse to −120 mV (Fig. 12).

i_h is reversibly blocked by millimolar concentrations of Cs^+ (Fig. 11*A*). Ba^{2+}, which is known to block other inward rectifying currents (Benson and Levitan 1983; Uchimura et al. 1989), is less effective, as 12.5 mM Ba^{2+} is not enough to block i_h completely, whereas 5 mM Cs^+ is sufficient.

The presence of a Ca^{2+}-activated current indicates the presence of a Ca^{2+} current. However, under our control conditions (TTX, PTX, and the rest of the currents intact) an inward current is not observed (see for example Fig. 4). To visualize small inward currents, the larger outward currents must be blocked. We used two methods for this purpose: *1*) iontophoretic injection of Cs^+ into the cell; and *2*) adding saturating concentrations of TEA to block $i_{o(Ca)}$ and a large fraction of i_d, and activating the current from a

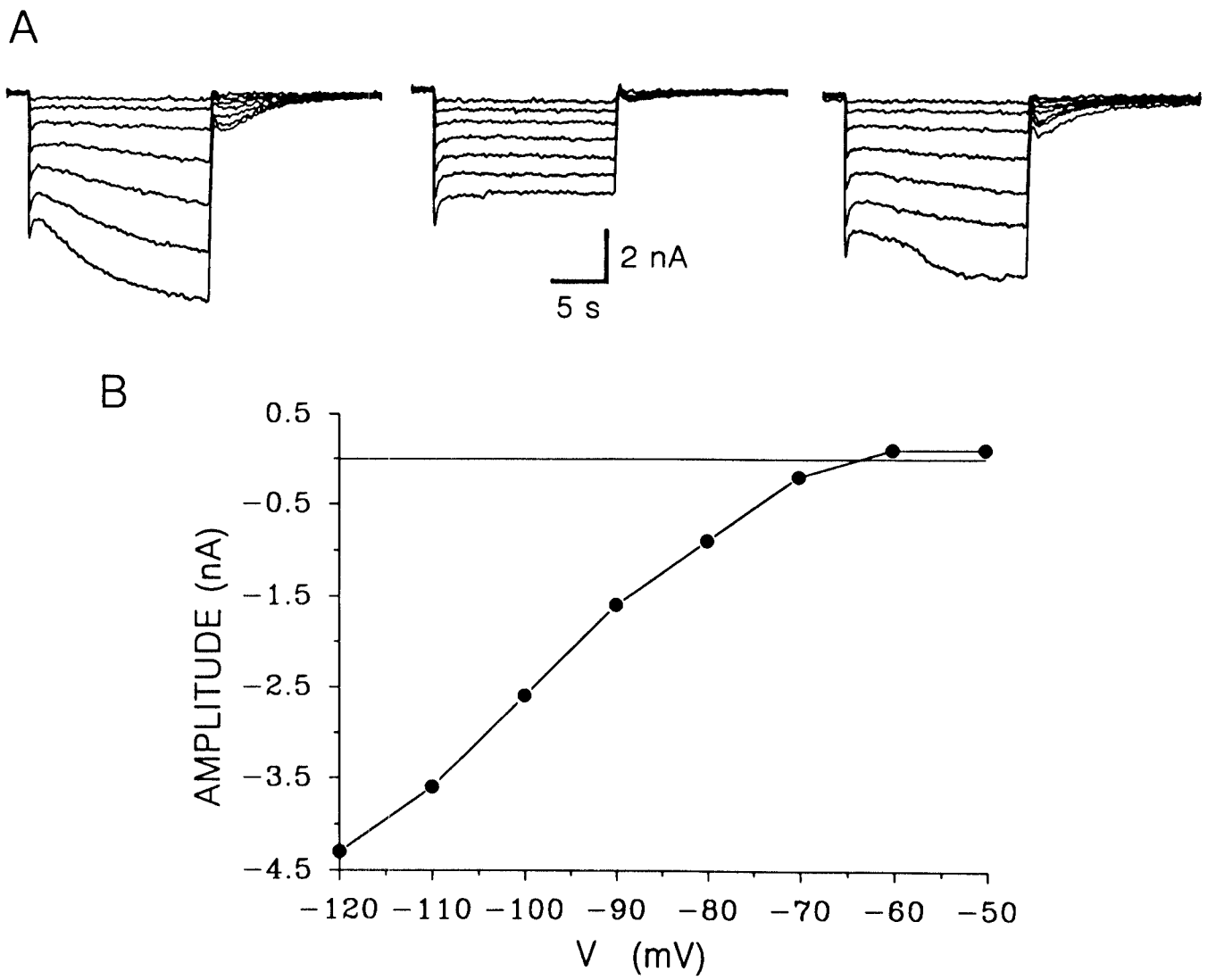

FIG. 11. i_h isolation, time course, and voltage dependence. LP cell in TEVC and TTX + PTX. *A*: voltage pulses from a $V_h = -40$ mV to a range between −110 and −50 mV. *Left*: control saline. *Middle*: in 5 mM Cs^+. *Right*: after 20 min washout of Cs^+. *B*: voltage dependence. *I-V* curve of the Cs^+-sensitive component obtained by subtraction of the currents measured in 5 mM Cs^+ from control saline in *A*. Measurements taken at the end of the 20-s-long pulses.

holding potential where i_A is inactive (e.g., $V_h = -40$ mV). By the use of the first of these methods (Fig. 13), a small inward current was revealed that activated at voltages more positive than −30 mV (Fig. 13*A*). Two hundred micromolars of Cd^{2+} blocks most of this current (Fig. 13*B*). Figure 14*A* displays the net Cd^{2+}-sensitive current obtained from data in Fig. 13, *A* and *B*. It shows the presence of apparently two components, a transient and a sustained component.

In most preparations Ba^{2+} both permeates better than Ca^{2+} through Ca^{2+} channels (Bean 1989) and fails to activate Ca^{2+}-activated K^+ currents. When Ba^{2+} was used as the charge carrier, an inward current was observed (Fig. 13*C*) that was also completely blocked by 200 μM Cd^{2+} (Fig. 13*D*), at least within the limits of the resolution of the present recording conditions. This Ba^{2+} current, like the Ca^{2+} current described above, was sensitive to Cd^{2+} and also shows two components: a transient one and a sustained component (Fig. 14*B*). This suggests that Ba^{2+} permeates through the same channels as Ca^{2+}.

With the use of $i_{o(Ca)}$ as an assay for i_{Ca}, we tested a number of blockers of known Ca^{2+} currents. Ten millimolars of Mn^{2+} and 10 mM Co^{2+} block $i_{o(Ca)}$ with an effectiveness similar to that of 200 μM Cd^{2+}. Fifty to two hundred millimolars of Ni^{2+}, which blocks some known Ca^{2+} currents (Susuki and Rogawski 1989; Tsien et al. 1988), did not affect $i_{o(Ca)}$. Finally, the dihydropyridine nifedipine, known to block a subclass of Ca^{2+} currents (Bean 1989; Susuki and Rogawski 1989; Tsien et al. 1988), had no apparent effect on i_{Ca}.

The TTX-sensitive Na^+ current underlying action-potential generation cannot be studied under somatic voltage clamp in the LP neuron. The action potentials are generated far enough from the cell body so that the spikes are attenuated in the soma (Fig. 3*A*) and are not subject to

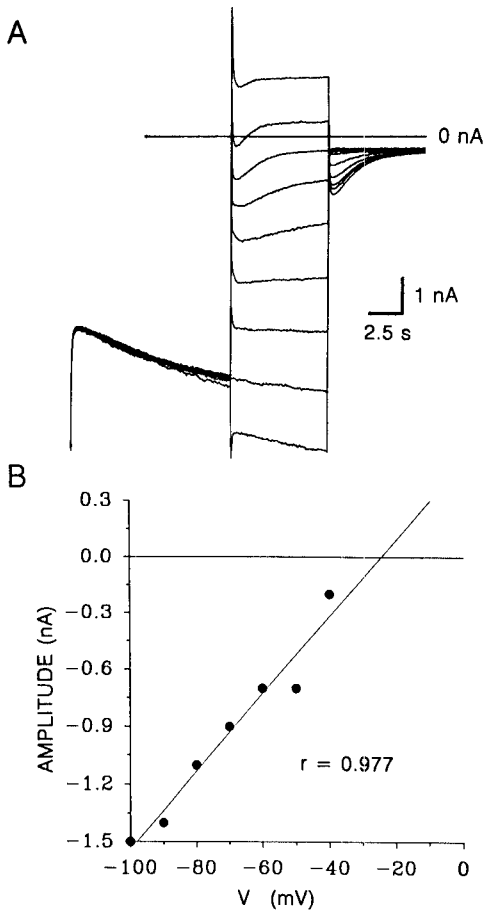

FIG. 12. i_h tail currents. LP cell in TEVC and TTX + PTX. *A*: protocol: the initial pulse to −110 mV was followed by a test pulse to a voltage varying from −120 mV (*bottom trace*) to −40 mV (*top trace*). V_h = −60 mV. *B*: tail currents measured like in *A*, at 200 ms after the onset of the test pulse, but with leak subtraction. For leak subtraction, a short, 200-ms pulse was applied to the same voltage range (−120 to −40 mV) without the prepulse to −110 mV. The extrapolation of the linear regression through the points indicates an $E_{rev} \approx -25$ mV.

voltage-clamp control. Action-potential generation is blocked by TTX or Saxitoxin (STX) at concentrations of 0.1 μM or higher but not affected by the presence of Cd^{2+}, TEA, Cs^+, or 4-AP.

DISCUSSION

The results presented here provide a first description of the major voltage-dependent ionic currents seen in the LP neuron of the crab STG. Obviously, we do not mean to imply that there are no additional currents to be recorded in these neurons. Indeed, it is likely that the modulatory inputs, the action of which we removed, might amplify or activate other currents that were undetectable under the conditions we employed. We anticipate that, as work on these currents continues, it may be possible to identify several different classes of Ca^{2+} currents or Ca^{2+}-activated currents. However, despite these caveats, we have been able to define those currents that are likely to contribute in a major way to the activity of the LP neuron, at least in the absence of exogenously applied neuromodulatory substances. Further work will be required to determine, for each of the many substances that can modulate the activity of the LP neuron (Golowasch and Marder 1992; Hooper and Marder 1987; Marder et al. 1986; Marder and Weimann 1992; unpublished observations; Nusbaum and Marder 1988, 1989a,b), the currents that each activates or influences.

Outward currents

We have identified three main outward currents that activate at membrane potentials more positive than V_{rest} (−49 mV, Table 1): a delayed rectifier-like current, an A-like current, and at least one type of Ca^{2+}-dependent outward current.

We argue that i_d, $i_{o(Ca)}$, and i_A are K^+ currents, or at least predominantly carried by K^+ for several reasons. The pharmacology of these currents is consistent with that of well-known K^+ currents of a number of different species. Although we would have liked to measure the actual reversal potential of these currents from tail current measurements and study its dependence on extracellular K^+, the large capacitance of our neurons made this impossible because we were unable to clamp the voltage during the initial 10–20 ms after an abrupt potential change (see Fig. 4), and tail currents have substantially decreased by 20 ms after the pulse. Nevertheless, we tried to determine the reversal potentials of these currents by using tail currents of total currents measured 20 ms after the voltage pulse. These tail currents were sensitive to extracellular $[K^+]$ and changed in the direction expected from the Nernst equation for K^+ (not shown). However, because we cannot determine the ionic selectivity of all the outward currents individually, for the calculation of maximum chord conductances we have assumed a reversal potential equal to a K^+ equilibrium potential of −80 mV for all three outward currents. This value for the K^+ equilibrium potential is taken from the fact that a γ-aminobutyric acid (GABA)-activated K^+ response in the same cell, with a reversal potential between −80 and −90 mV, behaves as a K^+ electrode (Marder and Paupardin-Tritsch 1978; Golowasch 1990).

The Ca^{2+}-dependent inactivation of $i_{o(Ca)}$ at high intracellular Ca^{2+} concentrations is interesting. By analogy with the Ca^{2+} block of Ca^{2+} currents (cf. Morad et al. 1988), it would suggest that Ca^{2+} can bind to the intracellular face of the pore of the channels underlying $i_{o(Ca)}$, thus reducing K^+ flux through them, and perhaps even permeate through them (Tsien et al. 1987).

Interestingly, cells from other related decapod crustaceans such as the lobster *Panulirus interruptus* (Graubard and Hartline 1988, 1991) and the lobster *Homarus americanus* (Tasaki and Cooke 1986) exhibit the same three outward currents as those here described for *C. borealis*, albeit with some differences.

1) In *C. borealis*, i_d is partially and reversibly blocked by TEA, similarly to what is seen in the lobster *H. americanus* (Tasaki and Cooke 1986) as well as a number of other preparations (Cobbett et al. 1989; Frech et al. 1989; Jones and Adams 1987; Thompson 1977). As in these cases, the estimated K_d varied between 0.5 and 1 mM, and, as in other

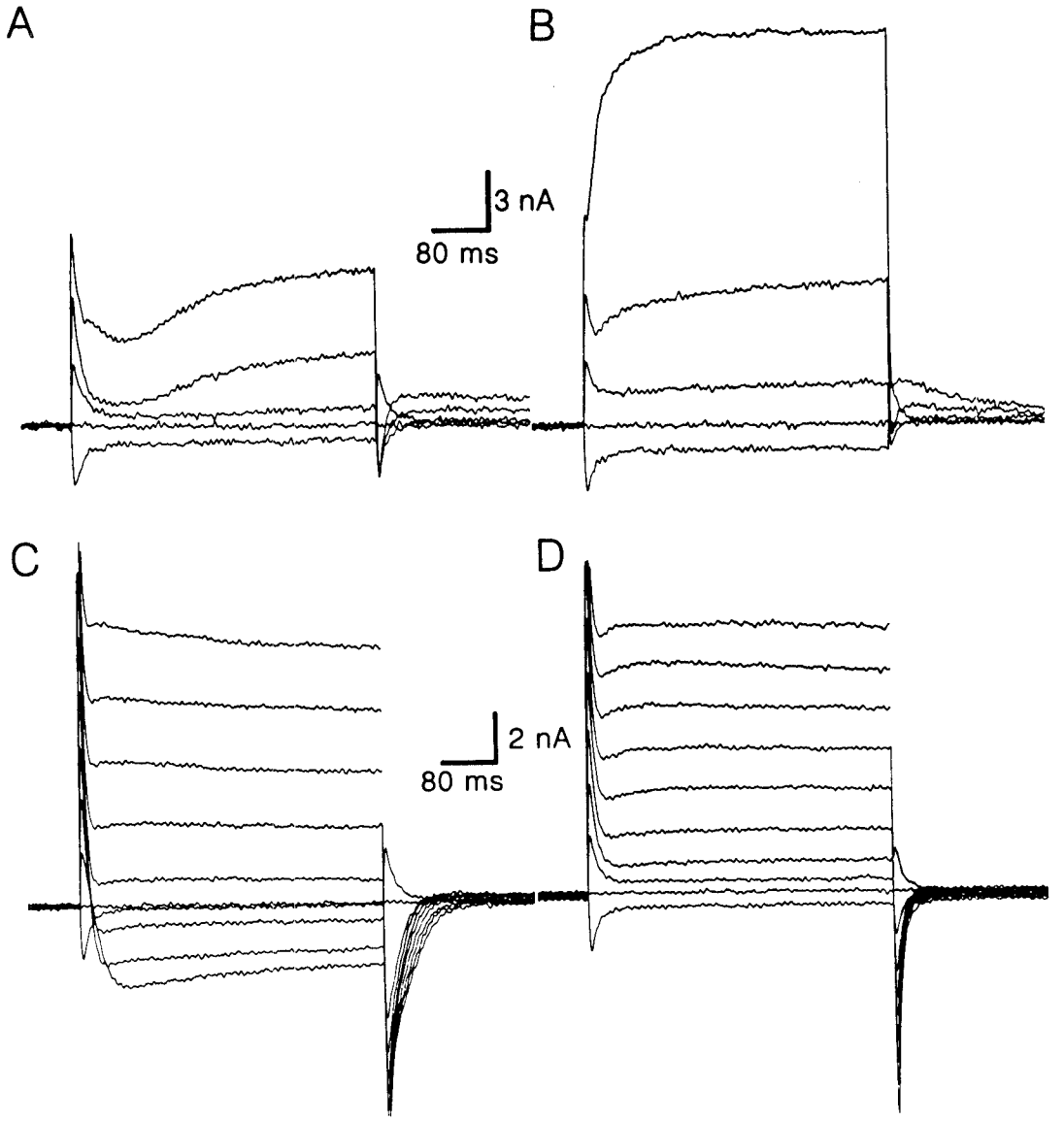

FIG. 13. Ca^{2+} current activation. LP cell in TEVC and TTX + PTX. Electrodes filled with 0.6 M Cs_2SO_4 + 20 mM KCl were employed. Cs^{2+} was iontophoresed into the cell during the course of ~3 h with depolarizing 500-ms pulses (1 Hz) of approximately +5 nA before recordings began. *A*: in control saline. Pulses from −50 to +10 mV. $V_h = -40$ mV. *B*: same cell as in *A* after addition of 200 μM Cd^{2+} in the bath. *C*: Ca^{2+} currents carried by Ba^{2+}. Different cell from that in *A* and *B*. Ninety-nine percent of the Ca^{2+} (12.9 mM) was substituted with Ba^{2+}. Pulses from −50 to +40 mV; $V_h = -40$ mV. *D*: same cell as in *C* after addition of 200 μM Cd^{2+} to the bath.

preparations, i_d is not affected by Cd^{2+} or by 4-AP. Furthermore, i_d has the typical delayed onset that becomes faster at more depolarized voltages (Fig. 5) that characterizes and defines the delayed rectifier currents.

2) i_A shows the typical voltage dependence of both activation and inactivation observed in other preparations: it usually activates at more positive voltages than V_{rest} but at more hyperpolarized voltages than does i_d (compare Figs. 5*B* and 9*B*), which is also seen in the lobsters *P. interruptus* (Graubard and Hartline 1991) and *H. americanus* (Tasaki and Cooke 1986) as well as a number of other cells (Cobbett et al. 1989; Neher 1971; Thompson 1977; Zbicz and Weight 1985). On the other hand, i_A inactivates at voltages below the threshold for its own activation (Fig. 9), although a small amount of overlap exists, similar to that observed in *H. americanus* (Tasaki and Cooke 1986) and other preparations (Connor 1975; Neher 1971; Zbicz and Weight 1985), so that the cell has to be held at a voltage lower than V_{rest} to allow the activation of this current with subsequent depolarizing pulses. The level of inactivation that can be released with hyperpolarization shows time and voltage dependence (Fig. 10), which is also characteristic of other described A-currents (Connor 1975; Neher 1971; Tasaki and Cooke 1986; Zbicz and Weight 1985).

i_A in the crab looks similar to the same current recorded in the cardiac ganglion of the lobster *H. americanus* (Tasaki and Cooke 1986). Some differences exist between i_A of *P. interruptus* (Graubard and Hartline 1991) and *C. borea-*

lis, namely that in *P. interruptus*, it is inactivated at −50 mV and the half inactivation voltage is −75 mV, whereas, in *C. borealis*, i_A is inactivated only ~85% at −50 mV, and the half inactivation voltage is −61 mV (Fig. 9, *C* and *D*). This implies that the activation and inactivation curves somewhat overlap in the crab's LP, whereas they do not in *P. interruptus* (Graubard and Hartline 1991). As described by Connor et al. (1977) for the walking leg axons of the crabs *Callinectes sapidus* and *Cancer magister*, i_A is somewhat different from the i_A here described for *C. borealis*. Although the activation and inactivation curves overlap substantially in *C. sapidus*' and *C. magister*'s axons, as in *C. borealis*' LP cell, they are shifted to more hyperpolarized voltages [compare our Fig. 9, *B* and *D*, with Fig. 3 in Connor et al. (1977)]. Interestingly, the walking leg axons show a baseline membrane potential around −60 to −70 mV during tonic action-potential firing, which coincides with the region where the activation and inactivation curves of i_A overlap. This allows i_A to have a noticeable influence on the spike rates of the leg axons (Connor et al. 1977). The LP cell's i_A activation and inactivation curves also overlap somewhat in the voltage range of the baseline of the tonically firing action potentials (Fig. 9, *B* and *D*). This suggests that i_A in the LP cell of *C. borealis* should also have some effect on the firing frequency of the cell (see Golowasch et al. 1992).

3) $i_{o(Ca)}$ is sensitive to divalent cations: Ca^{2+}, which activates it (Figs. 6, *A* and *C*, and 8), and Cd^{2+}, which blocks it (Fig. 6, *B* and *D*). As with other reported Ca^{2+}-activated K^+ currents (cf. Jones and Adams 1987; Pun and Behbehani 1990; Stanfield 1983; Zbicz and Weight 1985), $i_{o(Ca)}$ in *C. borealis* is sensitive to TEA. The sensitivity of this current to TEA contrasts sharply with that of the cells in the cardiac ganglion of *H. americanus*, where $i_{o(Ca)}$ is completely insensitive to TEA (named i_c by Tasaki and Cooke 1986) but is similar to the $i_{o(Ca)}$ of the STG cells of *P. interruptus* (Graubard and Hartline 1991).

We found that the maximum conductance ratios for the outward currents calculated from currents in the same cell are strikingly similar to the ratios of the averages of pooled maximum conductances from many different cells. This indicates that these currents adjust themselves to a constant relationship characteristic of the crab LP cell so that the LPs identity is reflected in the specific balance of conductances that produce its unique patterns of activity. This raises the fundamental question of what molecular mechanisms underly this balance of conductances.

Inward currents

The inwardly rectifying current found in the LP neuron resembles the i_h current described elsewhere (Angstadt and Calabrese 1989; Difrancesco 1986; DiFrancesco et al. 1986; DiFrancesco and Tromba 1988). It is activated by hyperpolarization, it is blocked by millimolar concentrations of Cs^+, and it reverses at voltages between −20 and −30 mV. However, the LP neuron's i_h is about an order of magnitude slower than that in the heart. A complication in the identification of this current is the fact that both Cs^+ and Ba^{2+} block it. The cardiac i_h is blocked only by Cs^+ (DiFrancesco and Noble 1989), whereas other inward rectifiers are blocked by both ions (Benson and Levitan 1983; Uchimura et al. 1989). However, the inward rectifier blocked by both Cs^+ and Ba^{2+} is a K^+ current (Benson and Levitan 1983; Uchimura et al. 1989), whereas the LP i_h is clearly not a K^+ current because its reversal potential is near −20 mV and E_K is close to −80 mV.

The Ca^{2+} current expressed by the LP cell appears to consist of two components: a transient and a sustained component (Figs. 13 and 14). Because both components are blocked by Cd^{2+}, it is possible that these two components reflect the activity of a current with complex kinetics and voltage dependence. Alternatively, there may be multiple Ca^{2+} currents that we have not been able to separate pharmacologically.

It is hard to fit the LP i_{Ca} into the currently accepted classification scheme of Ca^{2+} currents (T, L, and N type) (Bean 1989; Tsien et al. 1988). The block by Cd^{2+} and no effect of Ni^{2+} make it unlikely that our i_{Ca} is a T-type current. Moreover, the T-type current is a low-threshold activated current that is usually completely inactivated (Tsien et al. 1988) at the V_h used here to trigger the Ca^{2+} currents (Fig. 13). This rules out a low-threshold T-type current as the identity of the i_{Ca} we have thus far measured in the LP cell. We have seen no effect of bath applying the dihydropyridine antagonist, nifedipine, usually used to characterize the L-type Ca^{2+} current (Bean 1989; Susuki and Rogawski 1989; Tsien et al. 1988). Thus it seems that the Ca^{2+} current activated in the LP cell is a high-threshold

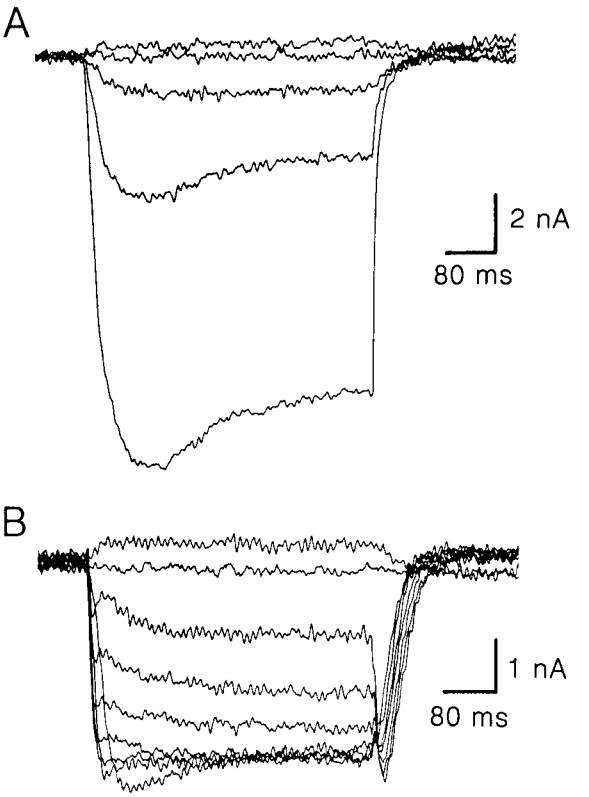

FIG. 14. Net Cd^{2+}-sensitive Ca^{2+} and Ba^{2+} currents. Data obtained from Fig. 13 by subtraction of currents obtained in the presence of 200 μM Cd^{2+} from control currents. *A*: Ca^{2+} currents. *B*: Ba^{2+} currents.

current with kinetics similar to those of the N and L types but with little or no dihydropyridine sensitivity.

Although the TTX-sensitive Na^+ current cannot be measured in the LP cell, its existence is evident because action potentials are readily abolished with 10^{-7}–10^{-6} M TTX or STX (see Fig. 2*C*).

The approach we have taken in this work differs from that taken by many biophysicists. Most often, cells are chosen for study because *1*) they are easy to voltage clamp, *2*) they provide a source of a particularly interesting and novel current, *3*) they have a particular current that is relatively easy to isolate because it is present in large amounts or activates in a voltage range significantly different from others, or *4*) they provide a cell in which a particular current's role in shaping the activity of the cell can be evaluated. The above strategy is obviously ideal for studying the properties of ion channels under optimal conditions. However, if one eventually wishes to understand how the neurons that participate in the generation of a specific behavior are modulated on the basis of their underlying currents, it is necessary to describe the currents in cells that are not ideally suited for the evaluation of all of their ionic currents, or possibly any of them. In recent years we are seeing more examples of attempts to characterize the currents that contribute to a neuron's electrical signature, or individual properties (Baxter and Byrne 1991; McCormick and Pape 1990; Susuki and Rogawski 1989; Yamada et al. 1989).

We argue that it is important to attempt to characterize the major components leading to the cell's electrical activity because the nonlinear voltage- and time-dependent processes in a neuron make it almost impossible to intuit what effects any one current will have on the behavior of a cell without an understanding of all of them, because any given current will play a different role depending on the constellation of currents giving rise to the dynamical properties of the neuron. For this reason, we have found it particularly useful to use models (Buchholtz et al. 1992; Golowasch et al. 1992) that incorporate the activity of these currents, to allow us to evaluate the role of each in the behavior of the neuron.

We thank Drs. John Lisman, Christopher Miller, Laurence Abbott, Michael Nusbaum, Terry Egan, Peter Reinhart, and Alfred Kirkwood for useful discussions through the course of this work. We are grateful for the helpful comments of the *Journal of Neurophysiology* reviewers.

This research was supported by National Institute of Neurological Disorders and Stroke Grant NS-17813.

J. Golowasch submitted part of this work in partial fulfillment of the requirements for the PhD in Biophysics at Brandeis University.

Present address of J. Golowasch: Laboratoire de Neurobiologie, Ecole Normale Supérieure, 46 rue d'Ulm, 75005 Paris, France.

Address reprint requests to E. Marder.

Received 31 May 1991; accepted in final form 4 September 1991.

REFERENCES

ADAMS, P. R., BROWN, D. A., AND CONSTANTI, A. M-currents and other potassium currents in bullfrog sympathetic neurones. *J. Physiol. Lond.* 330: 537–572, 1982.

ANGSTADT, J. D. AND CALABRESE, R. L. A hyperpolarization-activated inward current in heart interneurons of the medicinal leech. *J. Neurosci.* 9: 2846–2857, 1989.

ARBAS, E. A. AND CALABRESE, R. L. Ionic conductances underlying the activity of interneurons that control heartbeat in the medicinal leech. *J. Neurosci.* 7: 3945–3952, 1987.

BAXTER, D. A. AND BYRNE, J. H. Ionic conductance mechanisms contributing to the electrophysiological properties of neurons. *Curr. Opin. Neurobiol.* 1: 105–112, 1991.

BEAN, B. P. Classes of calcium channels in vertebrate cells. *Annu. Rev. Physiol.* 51: 367–384, 1989.

BENSON, J. A. AND LEVITAN, I. B. Serotonin increases an anomalously rectifying K^+ current in the *Aplysia* neuron R15. *Proc. Natl. Acad. Sci. USA* 80: 3522–3525, 1983.

BEZANILLA, F. AND ARMSTRONG, C. M. Inactivation of the sodium channel. I. Sodium current experiments. *J. Gen. Physiol.* 70: 549–566, 1977.

BUCHHOLTZ, F., GOLOWASCH, J., EPSTEIN, I. R., AND MARDER, E. Mathematical model of an identified stomatogastric ganglion neuron. *J. Neurophysiol.* 67: 332–340, 1992.

COBBETT, P., LEGENDRE, P., AND MASON, W. T. Characterization of three types of potassium currents in cultured neurons of rat supraoptic nucleus area. *J. Physiol. Lond.* 410: 443–462, 1989.

CONNOR, J. A. Neural repetitive firing: a comparative study of membrane properties of crustacean walking leg axons. *J. Neurophysiol.* 38: 922–932, 1975.

CONNOR, J. A. AND STEVENS, C. F. Voltage clamp studies of a transient outward current in gastropod neural somata. *J. Physiol. Lond.* 213: 21–30, 1971.

CONNOR, J. A., WALTER, D., AND MCKOWN, R. Neural repetitive firing. Modifications of the Hodgkin-Huxley axon suggested by experimental results from crustacean axons. *Biophys. J.* 18: 81–102, 1977.

CZTERNASTY, G., KADO, R. T., AND BRUNER, J. Analysis of mechanisms of spiking in normally 'non-spiking' motoneurone somata in crayfish. *J. Exp. Biol.* 147: 91–110, 1989.

DIFRANCESCO, D. Characterization of single pacemaker channels in cardiac sino-atrial node cells. *Nature Lond.* 324: 470–473, 1986.

DIFRANCESCO, D., FERRONI, A., MAZZANTI, M., AND TROMBA, C. Properties of the hyperpolarizing-activated current (i_f) in cells isolated from the rabbit sino-atrial node. *J. Physiol. Lond.* 377: 61–88, 1986.

DIFRANCESCO, D. AND NOBLE, D., Current i_f and its contribution to cardiac pacemaking. In: *Neuronal and Cellular Oscillators,* edited by J. W. Jacklet. New York: Dekker, 1989, p. 31–57.

DIFRANCESCO, D. AND TROMBA, C. Inhibition of the hyperpolarization-activated current (i_f) induced by acetylcholine in rabbit sino-atrial node myocytes. *J. Physiol. Lond.* 405: 477–491, 1988.

EDMAN, Å., GESTRELIUS, S., AND GRAMPP, W. Current activation by membrane hyperpolarization in the slowly adapting lobster stretch receptor neurone. *J. Physiol. Lond.* 384: 671–690, 1987.

EISEN, J. S. AND MARDER, E. Mechanisms underlying pattern generation in lobster stomatogastric ganglion as determined by selective inactivation of identified neurons. III. Synaptic connections of electrically coupled pyloric neurons. *J. Neurophysiol.* 48: 1392–1415, 1982.

FRECH, G. C., VANDONGEN, A. M. J., SCHUSTER, G., BROWN, A. M., AND JOHO, R. H. A novel potassium channel with delayed rectifier properties isolated from rat brain by expression cloning. *Nature Lond.* 340: 642–645, 1989.

GOLOWASCH, J. *Characterization of a Stomatogastric Ganglion Neuron. A Biophysical and a Mathematical Description* (PhD dissertation). Waltham, MA: Brandeis Univ., 1990.

GOLOWASCH, J., BUCHHOLTZ, F., EPSTEIN, I. R., AND MARDER, E. Contribution of individual ionic currents to activity of a model stomatogastric ganglion neuron. *J. Neurophysiol.* 67: 341–349, 1992.

GOLOWASCH, J. AND MARDER, E. Proctolin activates an inward current whose voltage dependence is modified by extracellular Ca^{2+}. *J. Neurosci.* In press.

GRAUBARD, K. AND CALVIN, W. H. Presynaptic dendrites: implications of spikeless synaptic transmission and dendritic geometry. In: *Neurosciences: IV Study Program,* edited by F. O. Schmitt and F. G. Worden. Cambridge, MA: MIT Press, 1979.

GRAUBARD, K. AND HARTLINE, D. K. Localization of currents in stomatogastric neurons. *Soc. Neurosci. Abstr.* 14: 296, 1988.

GRAUBARD, K. AND HARTLINE, D. K. Voltage clamp analysis of intact stomatogastric neurons. *Brain Res.* 557: 241–254, 1991.

HILLE, B. *Ionic Channels of Excitable Membranes.* Sunderland, MA: Sinauer, 1984.

HODGKIN, A. L. AND HUXLEY, A. F. A quantitative description of membrane current and its application to conduction and excitation in nerve. *J. Physiol. Lond.* 117: 500–544, 1952.

HOOPER, S. L. AND MARDER, E. Modulation of the lobster pyloric rhythm by the peptide proctolin. *J. Neurosci.* 7: 2097–2112, 1987.

HOOPER, S. L., O'NEIL, M. B., WAGNER, R., EWER, J., GOLOWASCH, J., AND MARDER, E. The innervation of the pyloric region of the crab, *Cancer borealis:* homologous muscles in decapod species are differently innervated. *J. Comp. Physiol. A Sens. Neural Behav. Physiol.* 159: 227–240, 1986.

JONES, S. W. AND ADAMS, P. R. The M-current and other potassium currents of vertebrate neurons. In: *Neuromodulation,* edited by L. Kaczmarek and I. Levitan. London: Oxford Univ. Press, 1987, p. 159–186.

KACZMAREK, L. AND LEVITAN, I. B. *Neuromodulation.* London: Oxford Univ. Press, 1987.

KNÖPFEL, T., VRANESIC, I., GÄHWILER, B. H., AND BROWN, D. A. Muscarinic and β-adrenergic depression of the slow Ca^{2+}-activated potassium conductance in hippocampal CA3 pyramidal cells in rest mediated by a reduction of depolarization-induced cytosolic Ca^{2+} transients. *Proc. Natl. Acad. Sci. USA* 87: 4083–4087, 1990.

LATORRE, R., OBERHAUSER, A., LABARCA, P., AND ALVAREZ, O. Varieties of calcium-activated potassium channels. *Annu. Rev. Physiol.* 51: 385–399, 1989.

MARDER, E. AND EISEN, J. S. Transmitter identification of pyloric neurons: electrically coupled neurons use different transmitters. *J. Neurophysiol.* 51: 1345–1361, 1984.

MARDER, E., HOOPER, S. L., AND SIWICKI, K. K. Modulatory action and distribution of the neuropeptide proctolin in the crustacean stomatogastric nervous system. *J. Comp. Neurol.* 243: 454–467, 1986.

MARDER, E. AND PAUPARDIN-TRITSCH, D. The pharmacological properties of some crustacean neuronal acetylcholine, γ-aminobutyric acid, and L-glutamate responses. *J. Physiol. Lond.* 280: 213–236, 1978.

MARDER, E. AND WEIMANN, J. M. Modulatory control of multiple task processing in the stomatogastric nervous system. In: *Neurobiology of Motor Programme Selection: New Approaches to Behavioral Choice,* edited by J. Kien, C. McCrohan, and W. Winlow. North Manchester, IN: Manchester Univ. Press. In press.

MCCORMICK, D. A. AND PAPE, H.-C. Properties of a hyperpolarization-activated cation current and its role in rhythmic oscillation in thalamic relay neurones. *J. Physiol. Lond.* 431: 291–318, 1990.

MORAD, M., DAVIES, N. W., KAPLAN, J. H., AND LUX, H. D. Inactivation and block of calcium channels by photo-released Ca^{2+} in dorsal root ganglion neurons. *Science Wash. DC* 241: 842–844, 1988.

NEHER, E. Two fast transient current components during voltage clamp of snail neurons. *J. Gen. Physiol.* 58: 36–53, 1971.

NUSBAUM, M. P. AND MARDER, E. A neuronal role for a crustacean red pigment concentrating hormone-like peptide: neuromodulation of the pyloric rhythm in the crab, *Cancer borealis. J. Exp. Biol.* 135: 165–181, 1988.

NUSBAUM, M. P. AND MARDER, E. A modulatory proctolin-containing neuron (MPN). I. Identification and characterization. *J. Neurosci.* 9: 1591–1599, 1989a.

NUSBAUM, M. P. AND MARDER, E. A modulatory proctolin-containing neuron (MPN). II. State-dependent modulation of rhythmic motor activity. *J. Neurosci.* 9: 1600–1607, 1989b.

PARKER, I. AND MILEDI, R. A calcium-independent chloride current activated by hyperpolarization in *Xenopus* oocytes. *Proc. R. Soc. Lond. B Biol. Sci.* 233: 191–199, 1988.

PUN, Y. K. AND BEHBEHANI, M. M. A rapidly inactivating Ca^{2+}-dependent K^+ current in pheochromocytoma cells (PC12) of the rat. *Pfluegers Arch.* 415: 425–432, 1990.

RALL, W. Core conductor theory and cable properties of neurons. In: *Handbook of Physiology. The Nervous System. Cellular Biology of Neurons.* Bethesda, MD: Am. Physiol. Soc., 1977, sect. 1, vol. I, part 1, chapt. 3, p. 39–97.

ROGAWSKI, M. A. The A-current: how ubiquitous a feature of excitable cells is it? *Trends Neurosci.* 8: 214–219, 1985.

SELVERSTON, A. I. AND MOULINS, M. (Editors). *The Crustacean Stomatogastric System.* Berlin: Springer-Verlag, 1987.

STANFIELD, P. R. Tetraethylammonium ions and the potassium permeability of excitable cells. *Rev. Physiol. Biochem. Pharmacol.* 97: 1–67, 1983.

SUSUKI, S. AND ROGAWSKI, M. A. T-type calcium channels mediate the transition between tonic and phasic firing in thalamic neurons. *Proc. Natl. Acad. Sci. USA* 86: 7228–7232, 1989.

TASAKI, K. AND COOKE, I. M. Currents under voltage clamp of burst-forming neurons of the cardiac ganglion of the lobster (*Homarus americanus*). *J. Neurophysiol.* 56: 1739–1762, 1986.

THOMPSON, S. H. Three pharmacologically distinct potassium channels in molluscan neurons. *J. Physiol. Lond.* 265: 465–488, 1977.

TSIEN, R. W., HESS, P., MCCLESKEY, E. W., AND ROSENBERG, R. L. Calcium channels: mechanisms of selectivity, permeation, and block. *Annu. Rev. Biophys. Chem.* 16: 265–290, 1987.

TSIEN, R. W., LIPSCOMBE, D., MADISON, D. V., BLEY, K. R., AND FOX, A. P. Multiple types of neuronal calcium channels and their selective modulation. *Trends Neurosci.* 11: 431–438, 1988.

UCHIMURA, N., CHERUBINI, E., AND NORTH, R. A. Inward rectification in rat nucleus accumbens neurons. *J. Neurophysiol.* 62: 1280–1286, 1989.

YAMADA, W. M., KOCH, C., AND ADAMS, P. Multiple channels and calcium dynamics. In: *Methods in Neuronal Modeling. From Synapses to Networks,* edited by C. Koch and I. Segev. Cambridge, MA: MIT Press, 1989, p. 97–134.

ZBICZ, K. L. AND WEIGHT, F. F. Transient voltage and calcium-dependent outward currents in hippocampal CA3 pyramidal neurons. *J. Neurophysiol.* 53: 1038–1058, 1985.